

Spectral CT imaging parameters and Ki-67 labeling index in lung adenocarcinoma

Mailin Chen, Xiaoting Li, Yiyuan Wei, Liping Qi, Ying-Shi Sun

Key Laboratory of Carcinogenesis and Translational Research (Ministry of Education/Beijing), Department of Radiology, Peking University Cancer Hospital & Institute, Beijing 100142, China

Correspondence to: Ying-Shi Sun. Key Laboratory of Carcinogenesis and Translational Research (Ministry of Education/Beijing), Department of Radiology, Peking University Cancer Hospital & Institute, No. 52 Fucheng Road, Haidian District, Beijing 100142, China. Email: sys27@163.com.

Abstract

Objective: To explore the correlation between the spectral computed tomography (CT) imaging parameters and the Ki-67 labeling index in lung adenocarcinoma.

Methods: Spectral CT imaging parameters [iodine concentrations of lesions (ICLs) in the arterial phase (ICLa) and venous phase (ICLv), normalized IC in the aorta (NICa/NICv), slope of the spectral HU curve (λ HUa/ λ HUv) and monochromatic CT number enhancement on 40 keV and 70 keV images (CT40keVa/v, CT70keVa/v)] in 34 lung adenocarcinomas were analyzed, and common molecular markers, including the Ki-67 labeling index, were detected with immunohistochemistry. Different Ki-67 labeling indexes were measured and grouped into four grades according to the number of positive-stained cells (grade 0, $\leq 1\%$; 1% < grade 1 $\leq 10\%$; 10% < grade 2 $\leq 30\%$; and grade 3, $> 30\%$). One-way analysis of variance (ANOVA) was used to compare the four different grades, and the Bonferroni method was used to correct the P value for multiple comparisons. A Spearman correlation analysis was performed to further research a quantitative correlation between the Ki-67 labeling index and spectral CT imaging parameters.

Results: CT40keVa, CT40keVv, CT70keVa and CT70keVv increased as the grade increased, and CT70keVa and CT70keVv were statistically significant ($P < 0.05$). These four parameters and the Ki-67 labeling index showed a moderate positive correlation with lung adenocarcinoma nodules. ICL, NIC and λ HU in the arterial and venous phases were not significantly different among the four grades.

Conclusions: The spectral CT imaging parameters CT40keVa, CT40keVv, CT70keVa and CT70keVv gradually increased with Ki-67 expression and showed a moderate positive correlation with lung adenocarcinomas. Therefore, spectral CT imaging parameter-enhanced monochromatic CT numbers at 70 keV may indicate the extent of proliferation of lung adenocarcinomas.

Keywords: Computed tomography; spectral CT; lung adenocarcinoma; Ki-67 labeling index

Submitted Oct 10, 2019. Accepted for publication Feb 10, 2020.

doi: 10.21147/j.issn.1000-9604.2020.01.11

View this article at: <https://doi.org/10.21147/j.issn.1000-9604.2020.01.11>

Introduction

A new international multidisciplinary classification of lung adenocarcinoma was proposed by the International Association for the Study of Lung Cancer (IASLC), the American Thoracic Society (ATS), and the European Respiratory Society (ERS) in 2011 (1) and adopted by the

World Health Organization (WHO) in 2015 (2) and widely used in China (3). Lung adenocarcinoma is classified into atypical adenomatous hyperplasia (AAH) and adenocarcinoma *in situ* (AIS), minimally invasive adenocarcinoma (MIA) and invasive adenocarcinoma (IAC) according to the nature of proliferation and invasion, with different prognoses. Thus, proliferation is a key feature for

the progression of lung adenocarcinoma, and the Ki-67 labeling index is a prognostic biomarker that is widely estimated by the immunohistochemical assessment of the nuclear antigen Ki-67. It has been demonstrated that proliferative activities determined by Ki-67 are correlated with the prognosis of lung cancer patients (4-8).

Traditional thin-section chest computed tomography (CT) is used to distinguish the invasiveness of lung adenocarcinoma by assessing morphological characteristics, including the size, margins (spur, lobulation), bubble lucency, ratio of ground glass nodules (GGNs), and solid proportion (9-16), and the size, ratio of GGNs and solid proportion are closely related to the prognosis of lung adenocarcinoma (10,16). Advances in our understanding of the pathologic and radiologic features of GGNs and an awareness of the significance of the CT attenuation number in assessing lung adenocarcinoma presented as GGNs were recently reported (17-19). Spectral CT imaging as a new quantitative tool is used to assess the perfusion of pulmonary parenchyma in patients with lung cancer (20). Spectral CT imaging parameters are more suitable or precise for quantifying the invasion of lung adenocarcinoma than traditional chest CT imaging parameters (21,22).

Thus, in the present study, we combined objective parameters obtained from spectral CT imaging with the Ki-67 labeling index to analyze their correlation and to predict the Ki-67 labeling index by spectral CT imaging parameters preoperatively.

Materials and methods

Patients

From January 2018 to August 2018, a total of 34 patients with 67 immunohistochemistry-proven lung adenocarcinomas (14 males, 20 females; age range, 45-81 years old; mean age, 61.5 ± 7.5 years old) were prospectively enrolled in the current study. This research protocol was approved by the Medical Ethical Committee of Peking University Cancer Hospital & Institute, and written informed consent was obtained from all patients in accordance with the guidelines of the National Health Commission of the People's Republic of China. Patients were selected for this investigation according to the following inclusion criteria: 1) the presence of a solitary lung adenocarcinoma proven by pathology and 2) no contraindications to the administration of iodinated

contrast material. Patients who did not undergo Ki-67 labeling index testing were excluded from this study.

CT examinations

CT examinations were performed with two-phase enhanced CT scanning using the spectral imaging mode on a Revolution Xstream CT scanner (GE Healthcare, WI, USA). The injection dose of iopromide (Ultravist 300; Bayer Schering Pharma AG, Guangzhou, China) was 40 mL (≤ 70 kg body weight) at a flow rate of 5 mL/s or 50 mL (> 70 kg body weight) at a flow rate of 6 mL/s, followed by 30 mL of saline solution at the same injection rate. With scan delays of 30 s and 90 s after the start of contrast injection, a gemstone spectral imaging (GSI) examination of the entire chest was performed during the arterial phase (AP) and portal venous phase (VP), respectively. There were no serious injection complications or issues in this study. Acquisition parameters included a tube current of 600 mA, a pixel matrix of 512x512, an SFOV of 500 mm, a collimation of 40 mm, a helical tube rotation time of 0.6 s, a helical pitch of 0.985, a slice thickness of 5 mm, and a slice gap of 5 mm. Then, 2.5- and 1.25-mm-thick contiguous axial images at default monochromatic energy levels of 40 KeV and 70 KeV were reconstructed with a soft tissue kernel (standard) with a GSI data file. The CT dose index volume (CTDIvol) for GSI acquisition was 4.73 mGy.

Quantitative analysis of spectral CT images

By using the GSI Volume Viewer software package at the AW4.7 workstation (GE HealthCare), we processed and analyzed all the previously acquired data. Monochromatic and material decomposition images were obtained by a chest radiologist with 10 years of experience to analyze the quantitative measurements. During data analysis, the radiologist made use of the display field of view (15 cm or 20 cm) to amplify the involved lesion of each image. The region of interest (ROI) was selected, and to avoid calcification, liquefaction, and necrosis and reduce noise (50 pixels), the ROI was moved away from pulmonary vessels and bronchi, made as large as possible at the maximum section of the lesion and placed in the largest area possible. All measurements were repeated three times at three contiguous imaging levels to ensure consistency, and the average values were analyzed.

Spectral curve images, monochromatic images at energy levels of 40 and 70 keV both in the AP (a) and VP (v) and

iodine-based material decomposition images were obtained from spectral CT acquisition for analysis. The iodine concentration of lesions (ICL_a/ICL_v) in the double-phase enhanced scan was measured in the iodine density image derived from the iodine/water-based material decomposition image. The iodine concentration in the descending aorta or subclavian artery (ICA) was also measured in the same slice. The normalized iodine concentration (NIC_a and NIC_v), which represents the ratio of iodine concentration in the lesion and descending aorta (NIC = ICL/ICA), was calculated. These iodine concentration parameters (i.e., ICL_a, ICL_v, ICA_a, ICA_v, NIC_a and NIC_v) were calculated both in the AP and VP. The slope of the spectral HU curve (λ HU) was assessed only in the 40–70 keV region by the equation λ HU = (CT_{40 keV}–CT_{70 keV}) HU/(70–40) based on previous studies. λ HU_a = (CT_{40 keV}_a–CT_{70 keV}_a) HU/(70–40) and λ HU_v = (CT_{40 keV}_v–CT_{70 keV}_v) HU/(70–40) were also calculated.

Pathological evaluation/detection of Ki-67 labeling index

Pathological specimens were routinely fixed in 10% formalin and paraffin embedded. Tissue sections, including the largest cut surface of the tumor, were cut at a thickness of 4 μ m and stained with hematoxylin and eosin (H&E). Pathological diagnoses were made by two experienced lung pathologists based on the new WHO histological classification of lung tumors in 2015 (5) as AAH, AIS, MIA and IAC.

Immunostaining was performed with the standard streptavidin-peroxidase (SP) technique with an antibody against Ki-67 (monoclonal mouse antibody MIB-1, 1:100 dilution). Tumor tissue sections underwent routine deparaffinization, dehydration, antigen repair, routine hematoxylin redyeing, dehydration, dimethylbenzene transparentization and gum mounting (22). Quantitative analyses of Ki-67 positive expression indicated by tan-stained particles located in the nucleus were performed and graded according to the number of positive-stained cells as follows: grade 0, $\leq 1\%$; 1% < grade 1 $\leq 10\%$; 10% < grade 2 $\leq 30\%$; and grade 3, $> 30\%$ (23,24). Moreover, immunohistochemical EnVision two-step staining was used to detect antibodies against P40, thyroid transcription factor-1 (TTF-1) and NapsinA.

Statistical analysis

Parameters are expressed as the $\bar{x} \pm s$ and are tested for

normal distribution using the Kolmogorov-Smirnov test. One-way analysis of variance (ANOVA) was used to compare quantitative parameters between grades 0, 1, 2, 3 and 4, and the Bonferroni method was used to correct the P value for multiple comparisons. A P value less than 0.05 indicated significance. Spearman correlation analysis was performed to further research the quantitative correlation between the Ki-67 labeling index and spectral CT imaging parameters as follows: 0–0.40, weakly correlated; 0.41–0.75, moderately correlated; 0.76–1.00, strongly correlated. SPSS software (Version 18.0; SPSS Inc., Chicago, IL, USA) was used to perform statistical analysis.

Results

Of the thirty-four patients, 1 had MIA (2.9%) and 33 had IAC (97.1%); there were 15 solid nodules and 19 GGNs, which presented as predominant lepidic growth in 9 cases, predominant acinar growth in 9 cases, solid growth in 2 cases, papillary growth in 2 cases, micropapillary growth in 1 case and infiltrating mucinous adenocarcinoma in 1 case; mixed growth was observed in 10 cases. All cases were confirmed by surgical pathology. Ki-67-positive cells were detected in 7 (20.6%) cases of grade 0, 15 (44.1%) cases of grade 1, 7 (20.6%) cases of grade 2 and 5 (14.7%) cases of grade 3.

Regarding the correlation between the Ki-67 labeling index and spectral CT imaging parameters, raw variables that showed an association are shown in Table 1. Based on the Spearman correlation analysis of the Ki-67 labeling

Table 1 Correlation between Ki-67 labeling index and spectral CT imaging parameters of lung adenocarcinoma

Parameters	Spearman correlation coefficient	P
Ki-67	1	–
CT _{40keV} _a	0.431	0.020
CT _{70keV} _a	0.454	0.013
ICL _a	0.114	0.558
NIC _a	–0.056	0.773
λ HU _a	0.098	0.611
CT _{40keV} _v	0.407	0.028
CT _{70keV} _v	0.442	0.016
ICL _v	–0.127	0.510
NIC _v	–0.117	0.546
λ HU _v	–0.179	0.354

CT, computed tomography; a, arterial phase; v, venous phase; ICL, iodine concentrations of lesions; NIC, normalized iodine concentration; λ HU, slope of the spectral HU curve.

index, the correlation coefficients were 0.431, 0.454, 0.417 and 0.442 for CT40keVa (P=0.020), CT40keVv (P=0.028), CT70keVa (P=0.013), and CT70keVv (P=0.016), respectively, indicating moderate significant correlation between the Ki-67 labeling index and spectral CT imaging parameters.

The results of the comparison of CTkeV, ICL, NIC and λHU in the four groups based on the Ki-67 labeling index are shown in Table 2, Figure 1. In the general cohort, CT70keVa and CT70keVv were significantly different among the four groups, and the two parameters gradually increased as the grade increased (Figures 2–5 correspond to grades 0, 1, 2, and 3, respectively). The CT40keVa and CT40keVv values also gradually increased (CT40keVa: -221.75±252.99 vs. -43.25±229.31 vs. 53.50±242.68 vs. 152.11±26.71, P=0.056; CT40keVv: -194.69±239.27 vs. -25.81±197.38 vs. 46.84±234.74 vs. 137.13±24.03, P=0.072); however, the difference did not reach statistical significance.

The IC, NIC and λHU did not differ significantly between grades in either the AP or VP, nor did they exhibit a relationship with the Ki-67 labeling index.

Discussion

Currently, although extensive studies have been conducted on the traditional chest CT features of lung adenocarcinomas, little is known about the relationship between spectral CT imaging parameters and molecular pathological markers such as the proliferative marker Ki-67 (24). The Ki-67 protein was originally defined by the

prototype monoclonal antibody Ki-67 (25), which was developed by immunizing mice with nuclei of the Hodgkin lymphoma cell line L428, and was expressed during all active phases of the cell cycle (G1, S, G2, and mitosis) except for G0 (resting cells); therefore, it is an excellent biomarker for predicting the alleged growth fraction of a given cell population (26). High proliferation is a property of cancer. Thus, the proliferative rate has been reported to predict poor survival in lung adenocarcinoma (23).

Nevertheless, the size, morphological characteristics and CT number of GGNs, to a certain extent, manifest the invasiveness of cancerous cells, similar to the Ki-67 labeling index in lung adenocarcinoma. Peng *et al.* (24) used three-dimensional CT imaging parameters (diameter, total volume, maximum CT number, average CT number and standard deviation of the CT number) to predict the Ki-67 labeling index preoperatively for the pathological assessment of GGNs and found that these CT imaging parameters increased significantly in the following order: AIS, MIA and IAC. The Ki-67 labeling index in early lung adenocarcinoma presenting with GGNs can be predicted by three-dimensional CT imaging parameters for differential diagnosis. In this study, spectral CT imaging parameters (CT40keVa, CT40keVv, CT70keVa and CT70keVv) and the Ki-67 labeling index showed a moderate positive correlation in lung adenocarcinoma, and the spectral CT imaging parameters CT70keVa and CT70keVv were significantly increased as the Ki-67 labeling index increased. We believe that the association between spectral CT imaging parameters and the Ki-67 labeling index is biological and pathophysiological and thus

Table 2 Comparison of CTkeVa/v, ICLa/v, NICa/v and λHUa/v in four grades of Ki-67 labeling index (N=34)

Parameters	Ki-67 ($\bar{x}\pm s$)				P
	Grade 0 (n=7)	Grade 1 (n=15)	Grade 2 (n=7)	Grade 3 (n=5)	
CT40keVa	-221.75±252.99	-43.25±229.31	53.50±242.68	152.11±26.71	0.056
CT70keVa	-292.97±249.28	-117.57±204.45	-30.74±215.75	61.23±10.63	0.009
ICLa	12.56±3.93	12.86±8.07	14.79±8.02	16.16±3.45	0.539
NICa	0.49±0.31	0.45±0.39	0.27±0.15	0.43±0.24	0.542
λHUa	2.59±0.87	2.85±0.66	2.81±1.53	3.03±0.60	0.973
CT40keVv	-194.69±239.27	-25.81±197.38	46.84±234.74	137.13±24.03	0.072
CT70keVv	-294.13±250.95	-103.99±183.04	-36.62±216.91	53.31±9.04	0.016
ICLv	15.69±3.65	13.96±4.68	13.65±3.81	14.52±3.32	0.709
NICv	0.78±0.25	0.92±1.04	0.61±0.19	0.67±0.17	0.602
λHUv	3.26±1.19	2.83±0.99	2.78±0.98	2.79±0.71	0.856

CT, computed tomography; a, arterial phase; v, venous phase; ICL, iodine concentrations of lesions; NIC, normalized iodine concentration; λHU, slope of the spectral HU curve.

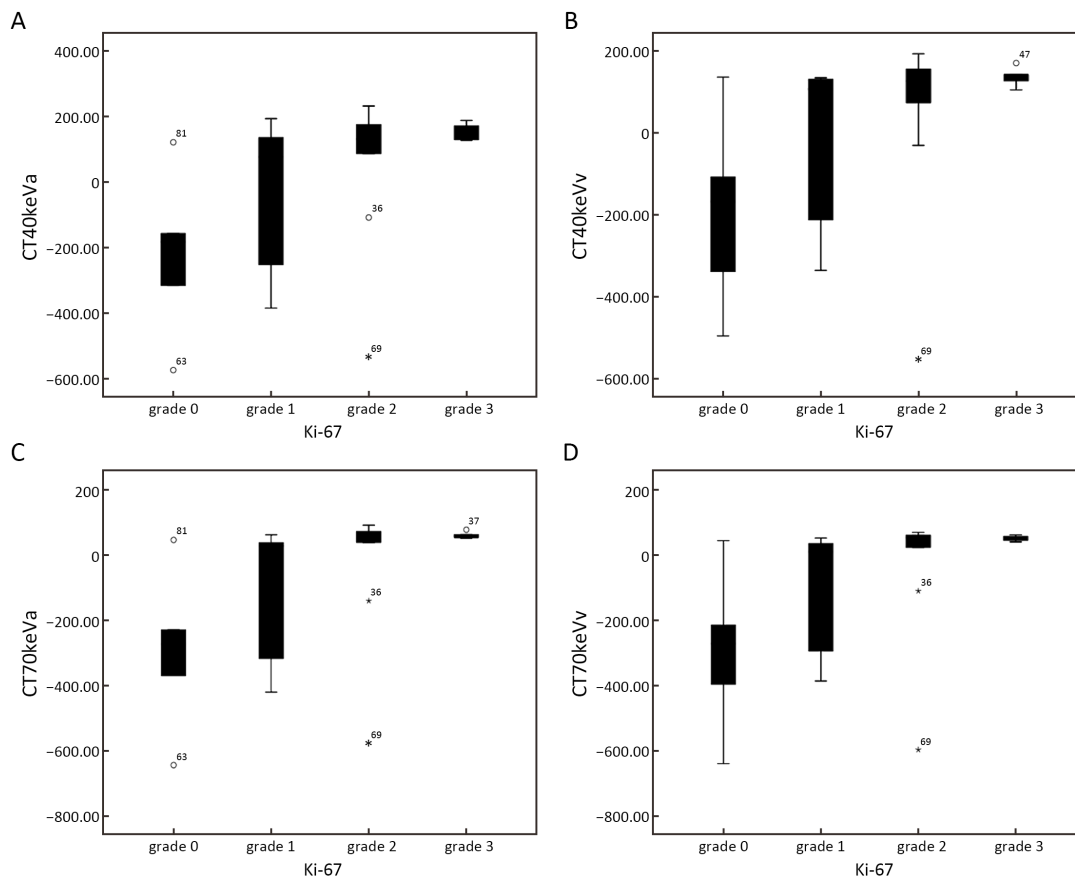


Figure 1 Comparison of spectral CT parameters in different grades of Ki-67 expression in lung adenocarcinoma. Values of CT40keVa ($P=0.056$) (A); CT40keVv ($P=0.072$) (B); CT70keVa ($P<0.05$) (C) and CT70keVv ($P<0.05$) (D) increased with the increase of Ki-67 expression, and only values of CT70keVa (C) and CT70keVv (D) showed statistical differences.

more than just statistical and mathematical.

The results of this study also confirmed the characteristics of hemodynamic changes in tumors. The more active the cell proliferation and growth are, the higher the Ki-67 index is, the higher the blood supply demand and new blood vessel formation are, and the higher the iodine-enhanced monochromatic CT value is. Therefore, spectral CT imaging parameters indirectly reflect the proliferation activity of lung adenocarcinoma.

Moreover, Peng *et al.* (24) reported that the Ki-67 labeling indexes of lesions presenting GGNs of different pathological categories are significantly different. If we could predict the Ki-67 labeling index before surgery, we could obtain a more accurate differential diagnosis of lung adenocarcinomas from not only radiology but also pathology. Thus, it may be helpful to evaluate the prognosis of lung adenocarcinomas if combined or complemented with the Ki-67 labeling index after surgery.

The main limitation of this study is the small sample size,

which leads to a relatively low precision of results. Further studies with a substantially larger number of patients are necessary to validate the present findings. Another potential limitation is that the prognoses of different subtypes of pulmonary lung adenocarcinoma vary greatly, and their spectral CT parameters and Ki-67 labeling index may be different. If we can compare these parameters in light of the different subtypes, the results may be more valuable. Last, the Ki-67 labeling index used for pathologic diagnosis was deliberately classified into four grades in a subjective manner to quantify the positive cell components by immunohistochemistry. However, we used different total doses of contrast medium and high-flow rates of injection to prevent possible bias.

Conclusions

This study underlines that the spectral CT imaging parameters CT40keVa, CT40keVv, CT70keVa and

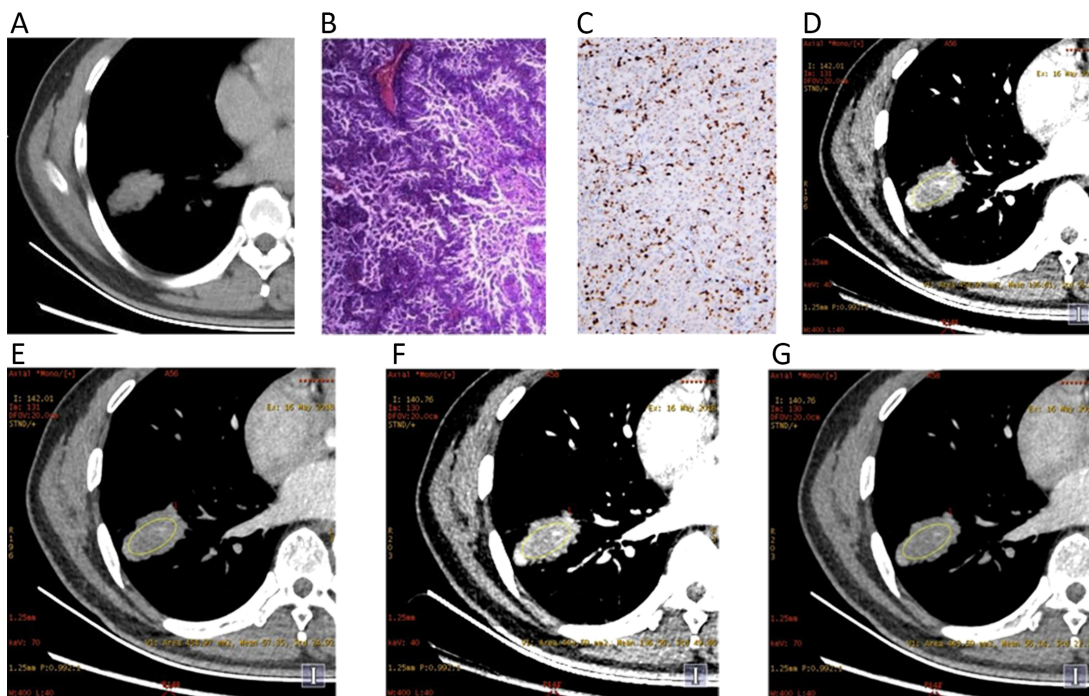


Figure 2 Spectral CT parameters in grade 3 of Ki-67 expression in lung adenocarcinoma. A 45-year-old male with right lower lung adenocarcinoma had 40% Ki-67 labeling index on conventional CT (A); pathological section (400×) (B); Ki-67 labeling index (400×) (C); CT40keVa (D); CT70keVa (E); CT40keVv (F); CT70keVv (G). CT, computed tomography; a, arterial phase; v, venous phase.

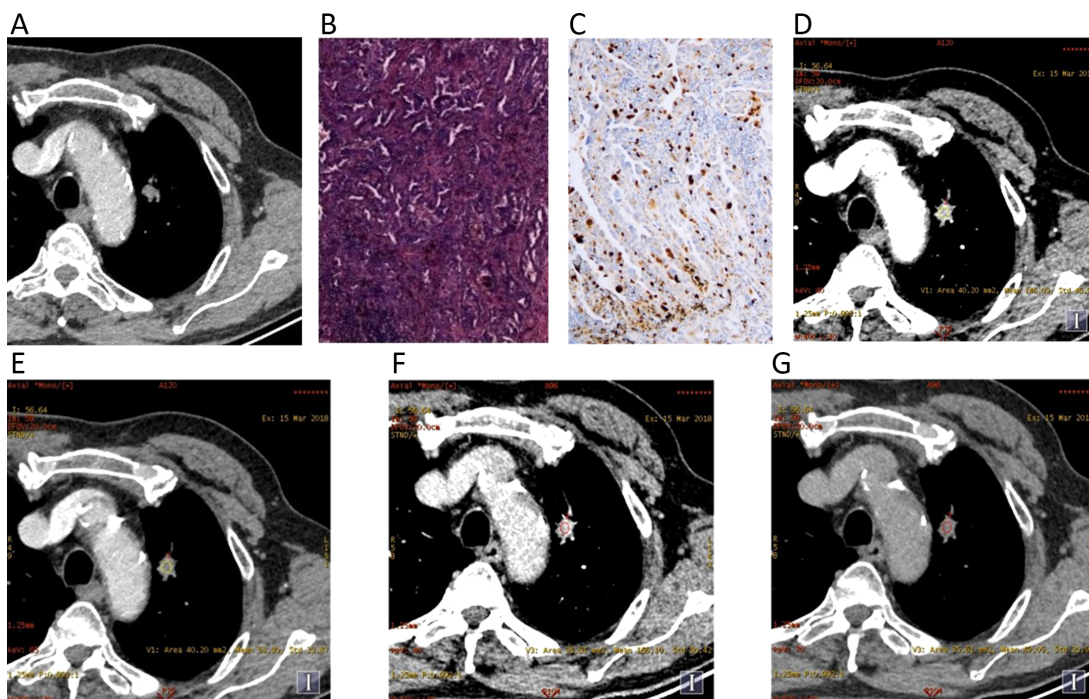


Figure 3 Spectral CT parameters in grade 2 of Ki-67 expression in lung adenocarcinoma. A 68-year-old male with lung adenocarcinoma had 20% Ki-67 labeling index on conventional CT (A); pathological section (B); Ki-67 labeling index (C); CT40keVa (D); CT70keVa (E); CT40keVv (F); CT70keVv (G). CT, computed tomography; a, arterial phase; v, venous phase.

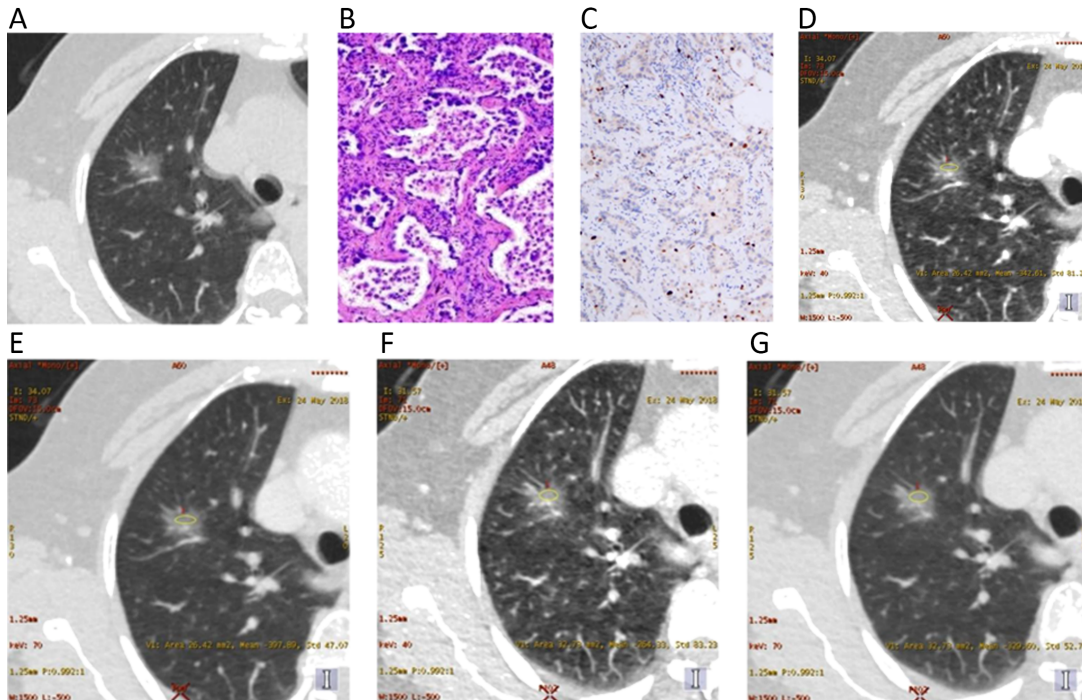


Figure 4 Spectral CT parameters in grade 1 of Ki-67 expression in lung adenocarcinoma. A 69-year-old female with lung adenocarcinoma had 5% Ki-67 labeling index on conventional CT (A); pathological section (400x) (B); Ki-67 labeling index (400x) (C); CT40keVa (D); CT70keVa (E); CT40keVv (F); CT70keVv (G). CT, computed tomography; a, arterial phase; v, venous phase.

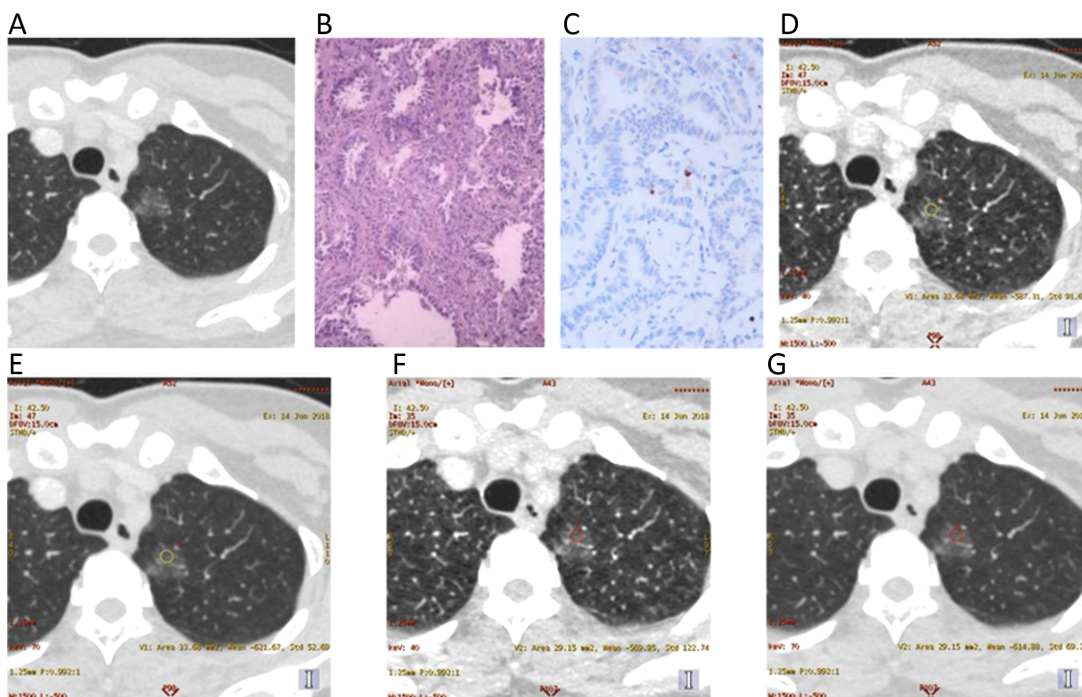


Figure 5 Spectral CT parameters in grade 0 of Ki-67 expression in lung adenocarcinoma. A 52-year-old female with lung adenocarcinoma had 1% Ki-67 labeling index on conventional CT (A); pathological section (400x) (B); Ki-67 labeling index (400x) (C); CT40keVa (D); CT70keVa (E); CT40keVv (F); CT70keVv (G). CT, computed tomography; a, arterial phase; v, venous phase.

CT70keVv show a moderate positive correlation with the Ki-67 labeling index, and CT70keVa and CT70keVv gradually increase with Ki-67 expression. Thus, these parameters could be used to predict the proliferation of lung adenocarcinoma.

Acknowledgements

This study was supported by National Natural Science Foundation of China (No. 91959116), Beijing Municipal Administration of Hospitals Clinical Medicine Development of Special Funding Support (No. ZYLX 201803), “Beijing Hospitals Authority” Ascent Plan (No. DFL20191103), and National Key R&D Program of China (No. 2017YFC1309101, 2017YFC1309104).

Footnote

Conflicts of Interest: The authors have no conflicts of interest to declare.

References

1. Travis WD, Brambilla E, Noguchi M, et al. International association for the study of lung cancer/American thoracic society/European respiratory society international multidisciplinary classification of lung adenocarcinoma. *J Thorac Oncol* 2011;6:244-85.
2. Travis WD, Brambilla E, Nicholson AG, et al. The 2015 World Health Organization Classification of Lung Tumors: Impact of Genetic, Clinical and Radiologic Advances Since the 2004 Classification. *J Thorac Oncol* 2015;10:1243-60.
3. Yang L, Wang N, Yuan Y, et al. Secular trends in incidence of lung cancer by histological type in Beijing, China, 2000–2016. *Chin J Cancer Res* 2019;31:306-15.
4. Ji Y, Zheng M, Ye S, et al. PTEN and Ki67 expression is associated with clinicopathologic features of non-small cell lung cancer. *J Biomed Res* 2014;28:462-7.
5. Berghoff AS, Ilhan-Mutlu A, Wöhrer A, et al. Prognostic significance of Ki67 proliferation index, HIF1 α index and microvascular density in patients with nonsmall cell lung cancer brain metastases. *Strahlenther Onkol* 2014;190:676-85.
6. Lei B, Liu S, Qi W, et al. PBK/TOPK expression in non-small-cell lung cancer: its correlation and prognostic significance with Ki67 and p53 expression. *Histopathology* 2013;63:696-703.
7. Ciancio N, Galasso MG, Campisi R, et al. Prognostic value of p53 and Ki67 expression in fiberoptic bronchial biopsies of patients with non-small cell lung cancer. *Multidiscip Respir Med* 2012;7:29.
8. Scagliotti GV, Micela M, Gubetta L, et al. Prognostic significance of Ki67 labelling in resected non-small cell lung cancer. *Eur J Cancer* 1993;29A:363-5.
9. Son JY, Lee HY, Lee KS, et al. Quantitative CT analysis of pulmonary ground-glass opacity nodules for the distinction of invasive adenocarcinoma from pre-invasive or minimally invasive adenocarcinoma. *PLoS One* 2014;9:e104066.
10. Lim HJ, Ahn S, Lee KS, et al. Persistent pure ground-glass opacity lung nodules ≥ 10 mm in diameter at CT scan: histopathologic comparisons and prognostic implications. *Chest* 2013;144:1291-9.
11. Si MJ, Tao XF, Du GY, et al. Thin-section computed tomography-histopathologic comparisons of pulmonary focal interstitial fibrosis, atypical adenomatous hyperplasia, adenocarcinoma *in situ*, and minimally invasive adenocarcinoma with pure ground-glass opacity. *Eur J Radiol* 2016;85:1708-15.
12. Moon Y, Sung SW, Lee KY, et al. Pure ground-glass opacity on chest computed tomography: predictive factors for invasive adenocarcinoma. *J Thorac Dis* 2016;8:1561-70.
13. Jin X, Zhao SH, Gao J, et al. CT characteristics and pathological implications of early stage (T1N0M0) lung adenocarcinoma with pure ground-glass opacity. *Eur Radiol* 2015;25:2532-40.
14. Ko JP, Suh J, Ibidapo O, et al. Lung adenocarcinoma: correlation of quantitative CT findings with pathologic findings. *Radiology* 2016;280:931-9.
15. Zhang Y, Tang J, Xu J, et al. Analysis of pulmonary pure ground-glass nodule in enhanced dual energy CT imaging for predicting invasive adenocarcinoma: comparing with conventional thin-section CT imaging. *J Thorac Dis* 2017;9:4967-78.
16. Takahashi M, Shigematsu Y, Ohta M, et al. Tumor invasiveness as defined by the newly proposed IASLC/ATS/ERS classification has prognostic significance for pathologic stage IA lung adenocarcinoma and can be predicted by radiologic parameters. *J Thorac*

- Cardiovasc Surg 2014;147:54-9.
17. Ikeda K, Awai K, Mori T, et al. Differential diagnosis of ground-glass opacity nodules: CT number analysis by three-dimensional computerized quantification. *Chest* 2007;132:984-90.
 18. Nomori H, Ohtsuka T, Naruke T, et al. Differentiating between atypical adenomatous hyperplasia and bronchioloalveolar carcinoma using the computed tomography number histogram. *Ann Thorac Surg* 2003;76:867-71.
 19. Nomori H, Ohtsuka T, Naruke T, et al. Histogram analysis of computed tomography numbers of clinical T1 N0 M0 lung adenocarcinoma, with special reference to lymph node metastasis and tumor invasiveness. *J Thorac Cardiovasc Surg* 2003;126:1584-9.
 20. Sun YS, Zhang XY, Cui Y, et al. Spectral CT imaging as a new quantitative tool? Assessment of perfusion defects of pulmonary parenchyma in patients with lung cancer. *Chin J Cancer Res* 2013;25:722-8.
 21. Zhang Y, Tang J, Xu J, et al. Analysis of pulmonary pure ground-glass nodule in enhanced dual energy CT imaging for predicting invasive adenocarcinoma: comparing with conventional thin-section CT imaging. *J Thorac Dis* 2017;9:4967-78.
 22. Son JY, Lee HY, Kim JH, et al. Quantitative CT analysis of pulmonary ground-glass opacity nodules for distinguishing invasive adenocarcinoma from non-invasive or minimally invasive adenocarcinoma: the added value of using iodine mapping. *Eur Radiol* 2016;26:43-54.
 23. Tabata K, Tanaka T, Hayashi T, et al. Ki-67 is a strong prognostic marker of lung adenocarcinoma when tissue heterogeneity is considered. *BMC Clin Pathol* 2014;14:23.
 24. Peng M, Peng F, Zhang C, et al. Preoperative prediction of Ki-67 labeling index by three-dimensional CT Image parameters for differential diagnosis of ground-glass opacity (GGO). *PLoS One* 2015;10:e0129206.
 25. Gerdes J, Schwab U, Lemke H, et al. Production of a mouse monoclonal antibody reactive with a human nuclear antigen associated with cell proliferation. *Int J Cancer* 1983;31:13-20.
 26. Scholzen T, Gerdes J. The Ki-67 protein: from the known and the unknown. *J Cell Physiol* 2000;182:311-22.

Cite this article as: Chen M, Li X, Wei Y, Qi L, Sun Y. Spectral CT imaging parameters and Ki-67 labeling index in lung adenocarcinoma. *Chin J Cancer Res* 2020;32(1):96-104. doi: 10.21147/j.issn.1000-9604.2020.01.11